



Contents lists available at ScienceDirect

## Progress in Oceanography

journal homepage: [www.elsevier.com/locate/pocean](http://www.elsevier.com/locate/pocean)

# Effect of CO<sub>2</sub> enrichment on phytoplankton photosynthesis in the North Atlantic sub-tropical gyre

Gavin Tilstone<sup>a,\*</sup>, Barbora Šedivá<sup>b</sup>, Glen Tarran<sup>a</sup>, Radek Kaňa<sup>b,c</sup>, Ondřej Prášil<sup>b,c</sup>

<sup>a</sup> Plymouth Marine Laboratory, Prospect Place, The Hoe, Plymouth PL1 3DH, UK

<sup>b</sup> Institute of Microbiology, Academy of Sciences of the Czech Republic, Opatovický mlyn, CZ-379 81 Třeboň, Czech Republic

<sup>c</sup> Faculty of Sciences, University of South Bohemia, Branišovská 31, 370 05 České Budějovice, Czech Republic

## ARTICLE INFO

## Article history:

Received 13 January 2016

Received in revised form 1 October 2016

Accepted 16 December 2016

Available online xxxx

## Keywords:

CO<sub>2</sub> enrichment

Picoeukaryotes

Dinoflagellates

Phytoplankton

Photosynthesis

Emission spectroscopy

Sub-tropical Atlantic Ocean

## ABSTRACT

The effects of changes in CO<sub>2</sub> concentration in seawater on phytoplankton community structure and photosynthesis were studied in the North Atlantic sub-tropical gyre. Three shipboard incubations were conducted for 48 h at ~760 ppm CO<sub>2</sub> and control (360 ppm CO<sub>2</sub>) from 49°N to 7°N during October and November 2010. Elevated CO<sub>2</sub> caused a decrease in pH to ~7.94 compared to ~8.27 in the control. During one experiment, the biomass of nano- and picoeukaryotes increased under CO<sub>2</sub> enrichment, but primary production decreased relative to the control. In two of the experiments the biomass was dominated by dinoflagellates, and there was a significant increase in the maximum photosynthetic rate ( $P_m^0$ ) and light-limited slope of photosynthesis ( $\alpha^0$ ) at CO<sub>2</sub> concentrations of 760 ppm relative to the controls. 77 K emission spectroscopy showed that the higher photosynthetic rates measured under CO<sub>2</sub> enrichment increased the connection of reversible photosystem antennae, which resulted in an increase in light harvesting efficiency and carbon fixation.

Crown Copyright © 2016 Published by Elsevier Ltd. All rights reserved.

## 1. Introduction

There is global concern over increases in the CO<sub>2</sub> concentration of seawater and the effects of ocean acidification on the functionality and productivity of marine ecosystems (Riebesell, 2008). Increases in atmospheric CO<sub>2</sub> from 280 to 370 ppm since the industrial revolution have decreased surface ocean pH by 0.12 units (Riebesell, 2004). The “business as usual” scenario predicts that CO<sub>2</sub> will rise to 700 ppm over the next 100 years (Houghton, 2001), which will decrease seawater pH by a further 0.3–0.6 units (Riebesell et al., 2007), bicarbonate ion (HCO<sub>3</sub><sup>-</sup>) concentration by 50% (Riebesell, 2004) and raise the sea surface temperature (SST) by 2–6 °C (Alley et al., 2007; Bopp et al., 2001). The projected pH shift from 8.2 to 7.7 covers the entire range of variation in pH currently observed in open ocean surface waters. The increase in SST is predicted to increase stratification and light availability of the surface ocean due to shoaling of the upper mixed layer (Rost et al., 2008; Sarmiento et al., 2004), which could directly impact the physiology of phytoplankton. These changes in pH, SST and light regime are predicted to enhance primary production (PP) (Hein and Sandjensen, 1997; Riebesell et al., 1993), especially in the North Atlantic (Bopp et al., 2001; Doney et al.,

2006; Feng et al., 2009), though this will depend on the associated dominant species and nutrient regime (Rost et al., 2008).

Information on the effects of CO<sub>2</sub> enrichment on phytoplankton photosynthesis in a range of organisms and different trophic systems is essential to understand potential shifts in the carbon cycle due to ocean acidification (Riebesell, 2004). Within the usual seawater pH range (8.0–8.3), 90% of the total DIC is HCO<sub>3</sub><sup>-</sup>, and CO<sub>2</sub> is less than 1% when the system is in equilibrium with atmospheric CO<sub>2</sub> (Skirrow, 1975). The total inorganic carbon concentration in seawater is 2 μmol L<sup>-1</sup> and the CO<sub>2</sub> content is 10 μmol L<sup>-1</sup>. This is not sufficient to saturate carbon fixation by the algal photosynthetic enzyme ribulose biphosphate carboxylase oxygenase (RuBisCO), which has half-saturation constants of 20–40 μmol L<sup>-1</sup> CO<sub>2</sub> for eukaryotic microalgae and up to 750 μmol L<sup>-1</sup> CO<sub>2</sub> for marine cyanobacteria (Badger et al., 1998; Hopkinson et al., 2011; Raven, 2011a; Raven and Johnston, 1991). Different phytoplankton groups or species have therefore evolved a preference for different forms of DIC, with some taking up CO<sub>2</sub> directly, whereas others draw on the pool of HCO<sub>3</sub><sup>-</sup> present (Elzenga et al., 2000) and or mechanisms to concentrate CO<sub>2</sub> or HCO<sub>3</sub><sup>-</sup>. Sensitivity to CO<sub>2</sub> therefore varies in relation to the HCO<sub>3</sub><sup>-</sup>:CO<sub>2</sub> preference and the affinity of phytoplankton for carbon fixation. Some species can rapidly acclimate to changes in the concentration of dissolved CO<sub>2</sub>, or total DIC (Nimer and Merrett, 1996). From an ecosystem perspective, it has been suggested that the responses of phytoplankton to reduced

\* Corresponding author.

E-mail address: [ghti@pml.ac.uk](mailto:ghti@pml.ac.uk) (G. Tilstone).

pH in a high CO<sub>2</sub> ocean are likely to be species-specific, with potential 'winners' and 'losers' (Hinga, 2002).

There is a growing body of literature on changes in photosynthesis due to increases in CO<sub>2</sub> and related effects (Brading et al., 2011; Feng et al., 2009, 2008; Flynn et al., 2015). The majority of studies have been conducted on phytoplankton in laboratory culture rather than on natural samples (Feng et al., 2008; Fu et al., 2007; King et al., 2015; Shi et al., 2015; Wu et al., 2010). In diatoms, some cyanobacteria and coccolithophorids, elevated CO<sub>2</sub> can lead to an increase in photosynthesis especially in large chain forming diatoms (Tortell and Morel, 2002; Tortell et al., 2008), *Synechococcus* spp. (Fu et al., 2007) and *Emiliania huxleyi* (Leonardos and Geider, 2005). In the diatom *Chaetoceros muelleri* for example, it has been shown that under saturating irradiance, maximal photosynthetic rates are stimulated by increasing CO<sub>2</sub> availability (Ihnen et al., 2011). For *Phaeodactylum tricoratum* grown at elevated CO<sub>2</sub> (1000 ppm) corresponding to 7.8 pH, there was greater photoinhibition of the electron transport rate from photosystem II (PSII) under high irradiance, whereas non-photochemical quenching was reduced compared to low CO<sub>2</sub> grown cells (Wu et al., 2010).

Most studies on natural samples in the Atlantic Ocean have been conducted in eutrophic and mesotrophic environments of the North Atlantic during natural or simulated blooms. Some of these report an increase in the abundance of diatoms compared to *Phaeocystis* spp. under CO<sub>2</sub> enrichment (Feng et al., 2008; Riebesell et al., 2007; Tortell et al., 2008), others report that nano-phytoplankton or Prymnesiophytes replace diatoms under elevated CO<sub>2</sub> and temperature in the Bering Sea (Hare et al., 2007) and the North Atlantic (Feng et al., 2008), where there was a change from diatoms to Prymnesiophytes under elevated CO<sub>2</sub> and a decrease in inorganic carbon production (calcification). There have been few studies of CO<sub>2</sub> enrichment on changes in phytoplankton community structure and photosynthesis in the oligotrophic gyres (Eggleston et al., 2010), even though they occupy the largest areas of the ocean. To date there has only been one study conducted in the sub-tropical North Atlantic at the Bermuda Atlantic Time Series site (BATS), which showed no significant difference in carbon fixation rates at elevated pCO<sub>2</sub> (reduced pH) for phytoplankton assemblages dominated by *Prochlorococcus* sp. and *Synechococcus* sp. (Lomas et al., 2012). By contrast, in the same study nitrogen fixation rates in colonies of *Trichodesmium* increased by 54% at pH 7.8 but decreased by 21% at pH 8.4.

The objective of this study was to assess the effect of CO<sub>2</sub> enrichment on phytoplankton photosynthesis and community composition in the North Atlantic sub-tropical gyre through a series of shipboard incubation experiments. Low temperature (LT) emission spectra were used to assess changes in major pigment-protein complexes in the oxygenic photosynthetic membranes. The LT spectra also provided information about the presence of chlorophyll-containing light harvesting antenna complexes and their functional coupling to photosystem reaction centres.

## 2. Methods

### 2.1. Study area and experimental design

Shipboard incubations were conducted aboard the *RRS James Cook* between 13 October and 21 November 2010 during the Atlantic Meridional Transect 20 (Cruise JC053). CO<sub>2</sub> enrichment experiments were carried out at three stations in the North Atlantic Gyre at 29°N, 34°W for experiment (Exp.) I; 18°N, 37°W for Exp. II and 7°N, 30°W for Exp. III (Fig. 1). For each Exp., 80 L of near surface seawater was collected from the ship's underway supply before dawn into a large Nalgene container. The water was sub-sampled

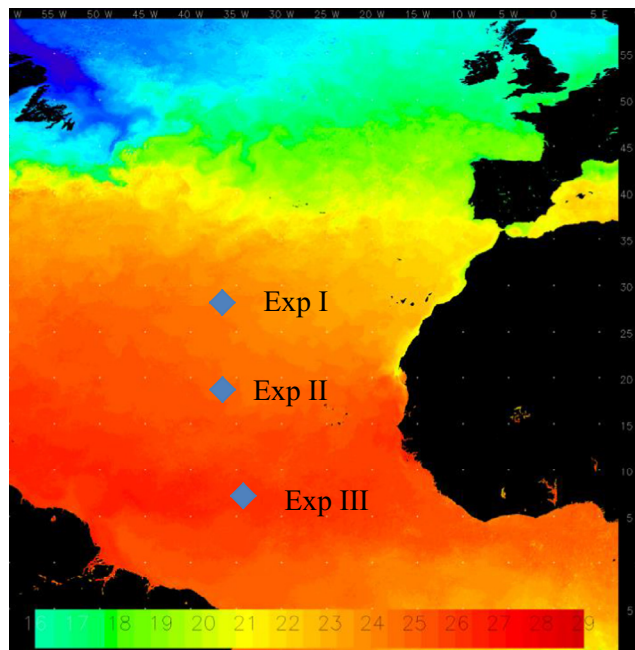


Fig. 1. Stations in the North Atlantic at which CO<sub>2</sub> enrichment experiments were conducted overlaid on MODIS-aqua Sea Surface Temperature monthly composite image for October 2010.

into 18 acid cleaned (IOC, 1994) 4 L clear polycarbonate bottles for incubation, leaving a head space of 0.5 L. Nine of the bottles were bubbled with pre-mixed synthetic air with 360 ppm CO<sub>2</sub> (control) and the other nine were bubbled with synthetic air with 760 ppm CO<sub>2</sub> (CO<sub>2</sub> treatment). The gases were supplied to the experimental bottles from gas cylinders via nylon tubing fitted with in-line 0.2 μm sterile Acrovent filters, to prevent contamination by particulates. The nylon tubing entered the bottles through Nalgene caps with Kinesis Omni-Lok fittings and vent tubes to prevent the build-up of pressure in the bottles. To minimise the effect of bubbling on phytoplankton, each experimental bottle was bubbled for an initial 8 h period followed by a further 4 h after 24 h to maintain the CO<sub>2</sub> over the 48 h period. The incubations were conducted in an on-deck incubation system (78 × 60 × 68 cm) supplied with flow through sub-surface seawater from the ship's underway supply to maintain the bottles at ambient temperature. The incubation system had no light screen, but the sides of the incubator were opaque which provided shading either side of zenith. pH, alkalinity, pCO<sub>2</sub>, HCO<sub>3</sub><sup>-</sup>, and Chl *a* were measured in triplicate at 0 (T0), 6, (T6; except Chl *a*), 12 (T12), 24 (T24) and 48 (T48) h. Samples for pico- and nanophytoplankton enumeration by flow cytometry, photosynthesis-irradiance curves and low emission spectra were measured in triplicate at T0, T24 and T48. Microscopy counts were made as single measurements at T0 and T48.

### 2.2. Carbonate chemistry: pH, pCO<sub>2</sub> and alkalinity

pH was determined spectrophotometrically onboard using 2 μmol L<sup>-1</sup> of mresol from a 2 mmol L<sup>-1</sup> stock solution which was prepared from pure sodium salt (Sigma-Aldrich, USA). This method expresses pH on the total hydrogen concentration scale with 0.01 precision (Dickson et al., 2003). Absorbance was recorded before and after addition of mresol at 434, 578 and 730 nm on a PerkinElmer Lambda 35 spectrophotometer in a 100 mm cuvette. Seawater temperature was measured using an Amarell Ama-Digit 15 Temperature probe, and salinity was taken

from a Seabird Electronics CTD calibrated against salinity standards. For total alkalinity, samples were stored in 100 mL borosilicate dark bottles with Teflon cap liners spiked with 5% mercuric chloride ( $6.9 \text{ nmol L}^{-1}$ ). Alkalinity was measured 2 months after the cruise using an automatic Apollo SciTech, Alkalinity Titrator (Model AS-ALK2) in  $0.8 \text{ M H}_2\text{SO}_4$ .  $\text{pCO}_2$  was calculated from the pH, temperature, salinity and alkalinity measurements using CO2SYS software (Pierrot and Wallace, 2006), using the constants set according to Mehrbach et al. (1973) and Dickson and Millero (1987) and corrected for differences between *in situ* and measured temperature.

### 2.3. Phytoplankton community structure

Nano and picoeukaryote phytoplankton cells from approx. 0.2 to  $10 \mu\text{m}$  were enumerated using a Becton Dickinson FACSort™ flow cytometer (Becton Dickinson, USA) equipped with an air-cooled laser providing blue light at 488 nm, using the methods given in Tarran et al. (2006, 2001). Picoeukaryotic phytoplankton and nanophytoplankton were analysed for between 2–4 min to measure chlorophyll fluorescence ( $>650 \text{ nm}$ ), phycoerythrin fluorescence ( $585 \pm 21 \text{ nm}$ ) and side scatter (light scattered at  $90^\circ$  to the plane of the laser). Using a combination of density plots as described in Tarran et al. (2001), it was possible to identify and quantify the following planktonic groups in the samples: *Prochlorococcus* spp., *Synechococcus* spp., picoeukaryotic phytoplankton (approx.  $0.6\text{--}3 \mu\text{m}$ , including prasinophyceae, chlorophyceae, pelagophyceae) and nanoeukaryotic phytoplankton (approx.  $3\text{--}10 \mu\text{m}$ , including cryptophyceae and prymnesiophyceae). Instrument flow rate was calibrated daily using Beckman Coulter Flowset fluorospheres of known concentration. Carbon biomass was calculated using median cell diameters measured for each group using the methods described in Tarran et al. (2006) and the carbon conversion factors given in Bjørnson (1986) and Booth (1988).

Microscopy was used to enumerate diatoms and dinoflagellates. For microscopic counts, 100 mL of seawater samples were collected into brown borosilicate bottles and preserved in Lugol's iodine (final concentration of 1%) for stations II and III. Dinoflagellates and diatoms were counted 2 months after the cruise using a Leica DM IRB microscope (Leica, Germany). 100 mL of sample was settled in composite sedimentation chambers for 24 h. Samples were counted on 26 mm diameter sedimentation slides in replicate vertical and horizontal transects using a  $\times 20$  objective. Cell volumes for these groups were calculated using approximate geometric shapes and converted to biomass using the equations given in Menden-Deuer and Lessard (2000).

For analysis of Chlorophyll-*a* (Chl *a*), 100 mL samples were filtered onto 25 mm GF/F filters (pore size  $0.7 \mu\text{m}$ , Whatman). The filter was then placed in a 15 mL Falcon™ tube (BD, UK) and 10 mL of 90% acetone was added. The tubes were then stored in the dark, in a  $-20^\circ \text{C}$  freezer for 12 h. Chl *a* was then measured onboard fluorometrically following Holm-Hansen et al. (1965) using a Turner Designs, Trilogy Fluorometer.

### 2.4. Phytoplankton photosynthesis

#### 2.4.1. Photosynthesis-irradiance curves

Photosynthetic-irradiance (P-E) experiments were conducted in linear photosynthetic irradiance illuminated with 50 W, 12 V tungsten halogen lamps following the methods described in Tilstone et al. (2003). Each incubator housed 16 sub-samples in 60 mL acid-cleaned polycarbonate bottles, which were inoculated with between 185 kBq ( $5 \mu\text{Ci}$ ) and 370 kBq ( $10 \mu\text{Ci}$ ) of  $^{14}\text{C}$  labelled bicarbonate. The PE curves were conducted at the same time each day to minimise the influence of diel light history. PAR in the incu-

ator was set to ambient levels measured over a 2 h period prior to incubation using a Skye Instruments PAR Sensor (model SKP 200). For Exps I, II and III these were 1319, 2166 and  $2215 \mu\text{E m}^{-2} \text{ s}^{-1}$ , respectively. The P-E curves were maintained at *in situ* temperature using the ship's non-toxic seawater supply. After 1.5 h incubation, the suspended material was filtered through 25 mm GF/F filters which were then exposed to 37% hydrochloric acid fumes for 12 h and then immersed in scintillation cocktail.  $^{14}\text{C}$  disintegration time per minute (DPM) was measured using the onboard 1414 liquid scintillation counter (PerkinElmer, USA) and the external standard and the channel ratio methods to correct for quenching. Dark  $^{14}\text{C}$  uptake was subtracted from light uptake in the other 15 light incubation cells. Photosynthetic rates were calculated from total dissolved inorganic carbon (DIC) and Chl *a*. DIC was calculated from salinity and alkalinity. The broadband light-saturated Chl-*a* specific rate of photosynthesis,  $P_m^B$  [ $\text{mg C (mg Chl } a)^{-1} \text{ h}^{-1}$ ], and the light-limited slope,  $\alpha^B$  [ $\text{mg C (mg Chl } a)^{-1} \text{ h}^{-1} (\mu\text{mol m}^{-2} \text{ s}^{-1})^{-1}$ ], were estimated by normalising  $^{14}\text{C}$  uptake to Chl *a* and fitting the data to the model of Platt et al. (1980). Primary production ( $\text{mg C m}^{-3} \text{ d}^{-1}$ ) was subsequently calculated from photosynthetically active radiation ( $E_{\text{PAR}}$ ), Chl *a* and the photosynthetic parameters using the brand model of Tilstone et al. (2003).  $E_{\text{PAR}}$  was modelled using the approach of Gregg and Carder (1990) modified to include the effects of clouds (Reed, 1977) and using wind speed and percentage cloud cover from the European Centre for Medium Range Weather Forecasting (ECMWF) following Smyth et al. (2005).

#### 2.4.2. Low temperature fluorescence emission spectra

Samples were filtered onto 25 mm GF/F filters from  $\sim 1 \text{ L}$  of sea water and processed following standard protocols (Suggett et al., 2009). A  $4 \times 10 \text{ mm}$  piece of the filter was cut and placed onto a holder, flash frozen in liquid nitrogen and measured immediately using a SM-9000 spectrometer (Photon Systems Instruments, Brno). The instrument is based on a Zeiss MCS CCD spectrometer; the detector has 1044 pixels, the grating images from 200 to 980 nm, the wavelength accuracy is 0.5 nm and the spectral resolution is 3.5 nm (FWHM). Two gaussian shaped lines are separated at  $>3.5 \text{ nm}$ , with a resolution of 3.2 nm from 0.8 nm dispersion by 4 pixels. Whole fluorescence emission spectra were determined using an integration time of 1000 ms. The fluorescence emission of blanks (seawater pre-filtered through a  $0.7 \mu\text{m}$  GF/F) was subtracted and the spectra were normalised to 686 nm for deconvolution (Kaňá et al., 2012).

### 2.5. CTD and nutrients

A Seabird 911 plus CTD was deployed at each station at which experiments were conducted. The data was processed using Seabird software v7.21 and up and down casts were then merged to 1 m binned resolution. Micro-molar nutrients were analysed using a 5 channel nitrate (Brewer and Riley, 1965), nitrite (Grasshoff, 1976), phosphate, silicate (Kirkwood, 1989) and ammonia (Mantoura and Woodward, 1983) Bran & Luebbe AIII segmented flow, colourimetric, autoanalyser. Water samples were taken from a  $24 \times 20 \text{ l}$  bottle stainless steel framed CTD/Rosette system (Seabird). These were sub-sampled into clean (acid-washed) 60 mL HDPE (Nalgene) sample bottles. Subsequent nutrient analysis was complete within 1–2 h of sampling. Clean handling techniques were employed to avoid contamination of the samples.

### 2.6. Statistical analysis

Paired *T*-tests samples were employed to test for significant differences between treatments at T48 on individual Exp.'s and for all

Exp.'s. Results of *T*-test analyses from all Exp.'s (I–III) at 48 h are given in Table 2. Results of *T*-test analyses from individual Exp.'s at 48 h are given on each sub-figure. The *T*-test results are given as  $T_{1,19} = x$  and  $P = y$  where *T* is the deviation of the sample mean from the normally distributed parametric mean to parametric standard deviation ratio, the sub-script numbers (1, 23) denote the degrees of freedom and *P* is the *T*-test critical significance value.

### 3. Results

#### 3.1. Initial hydrographic conditions

Temperature varied from 26 °C to 29 °C in the surface waters of the sub-tropical Atlantic (Figs. 1 and 2). These stations were typically oligotrophic with a deep thermocline at between 50 and 75 m, low nitrate and nitrite (<0.02 μM), low surface Chl *a* (0.03–0.05 mg m<sup>-3</sup>) and deep Chl *a* maxima between 70 and 130 m of between 0.1 and 0.3 mg m<sup>-3</sup> (Fig. 2B–D). The concentrations of nitrate + nitrite and silicate in the surface waters were beyond the detection limit (Harris, 2011).

#### 3.2. Changes in carbonate chemistry

For all experiments, by 48 h the CO<sub>2</sub> treatment resulted in an average concentration of 748 ppm and 7.97 pH units compared to 468 ppm and 8.14 pH units in the control (Fig. 3). For the control, bubbling pre-mixed synthetic air with a CO<sub>2</sub> concentration of 360 ppm to natural seawater, resulted in >460 ppm (Fig. 3). At 48 h the difference in CO<sub>2</sub> content and pH between the CO<sub>2</sub> treatment and control was ~280 ppm and 0.17 pH units, respectively (Fig. 3). Similarly, the mean HCO<sub>3</sub><sup>-</sup> in the CO<sub>2</sub> treatment during these Exp.'s was 2013 ppm and 1860 ppm in the control (Fig. 4A–C) and the mean HCO<sub>3</sub><sup>-</sup>:CO<sub>2</sub> ratio was 2.7 in the CO<sub>2</sub> treatment and 3.99 in the control (Fig. 4D–F).

The corresponding changes in total carbon (TC) and alkalinity (TA) during each experiment are given in Table 1. For all Exp.'s, the TA in the control and CO<sub>2</sub> enrichment was similar and conse-

quently there was no significant difference in TA for Exp. II & III and all Exp.'s together (Table 2). There was a significant difference in TA between CO<sub>2</sub> and control at T48 for Exp. I ( $T = 55.25$ ,  $P = 0.012$ ). By contrast, TC was significantly higher in the CO<sub>2</sub> treatment during Exp. II ( $T = 4.42$ ,  $P = 0.048$ ) & III ( $T = 7.08$ ,  $P = 0.019$ ) and all Exp.'s together (Table 2), but this was not significant for Exp. I. Carbonate chemistry in the bottles equilibrated at between 12 and 24 h. For all Exp.'s, there was a significant difference in CO<sub>2</sub>, pH, HCO<sub>3</sub><sup>-</sup> and HCO<sub>3</sub><sup>-</sup>:CO<sub>2</sub> TC, TA, (Table 2) between control and CO<sub>2</sub> treatments. At T48 in the CO<sub>2</sub> treatment, the CO<sub>2</sub> concentration was significantly higher than at T0 (Fig. 3; Table 2).

#### 3.3. Changes in phytoplankton community structure

During Exp.'s I & II there was no significant difference in Chl *a* between CO<sub>2</sub> and control treatments (Fig. 5) and as a consequence, for all Exp.'s. there was no significant difference between treatments and with T0 (Table 2). In Exp. III, Chl *a* was significantly higher in the control (Fig. 5C). Of the phytoplankton groups enumerated by flow cytometry, nanoeukaryotes had the highest biomass in Exp.'s I and II, whereas in Exp. III the biomass of nano- and picoeukaryotes and *Synechococcus* spp. were similar (Figs. 6 and 7). During all Exp.'s, there was no difference in nanoeukaryotes and picoeukaryotes between control and CO<sub>2</sub> treatments (Table 2). During Exp. I, there was little change in the biomass of nanoeukaryotes and picoeukaryotes over the duration of the Exp.'s and there was no significant difference between control and CO<sub>2</sub> treatment (Fig. 6A and D). During Exp. II, the initial biomass of nanoeukaryotes and picoeukaryotes decreased at 24 h followed by a slight increase at 48 h, but there was no significant difference in biomass between control and CO<sub>2</sub> treatments at 48 h (Fig. 6B and E). In Exp. III, the biomass of these groups initially decreased, but at 48 h both nanoeukaryotes and picoeukaryotes were significantly higher in the control compared to the CO<sub>2</sub> treatments and T0 (Fig. 6C and F). During all experiments there was no significant difference between control and CO<sub>2</sub> treatments for *Synechococcus* spp. and *Prochlorococcus* spp. (Fig. 7, Table 2). The biomass of *Prochlorococcus* spp. and *Synechococcus* spp. decreased

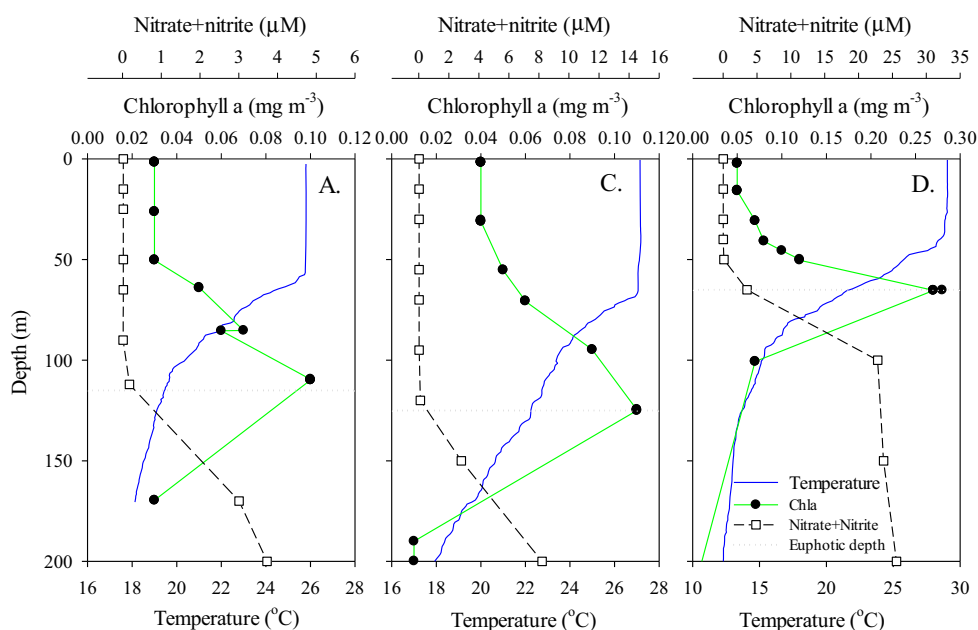


**Fig. 2.** Initial profiles of temperature (blue line), nitrate (black line, open squares) and chlorophyll *a* (green line, filled squares) at stations sampled for the CO<sub>2</sub> enrichment experiments (A) I, (B) II, (C) III. Dotted line is the euphotic depth. (For interpretation of the references to colour in this figure legend, the reader is referred to the web version of this article.)

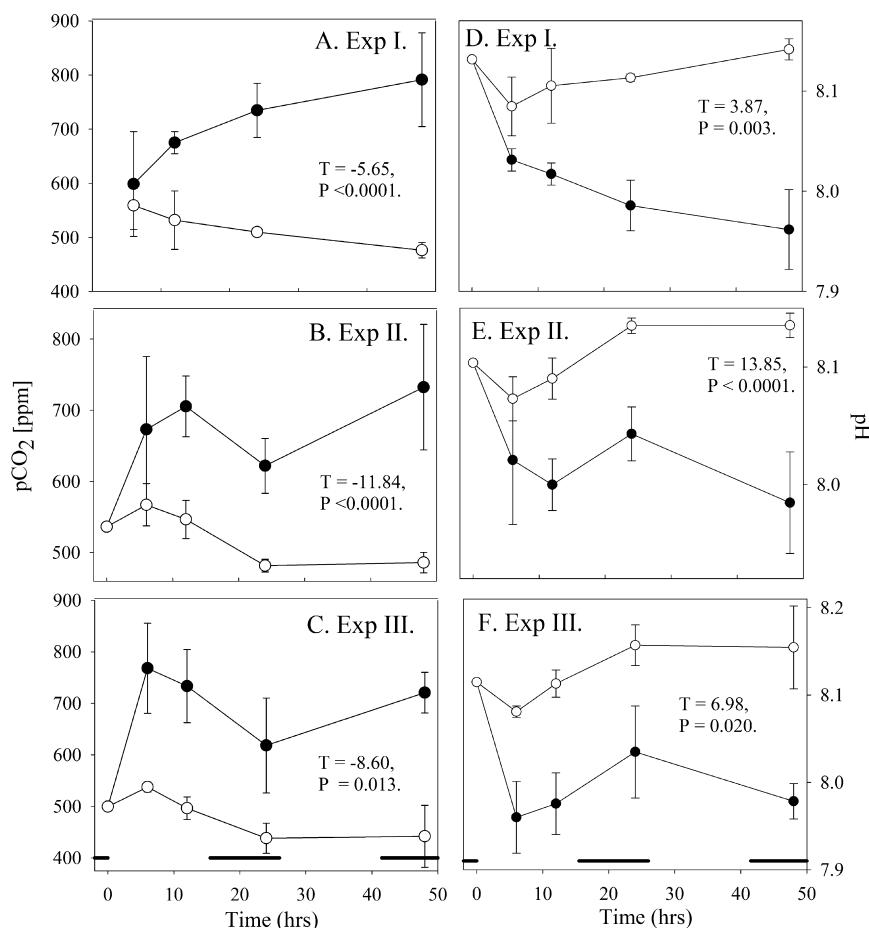


**Fig. 3.** Changes in pCO<sub>2</sub> during experiments (A) I, (B) II, (C) III, and in pH during experiments (D) I, (E) II, (F) III in control (open circles) and 760 ppm CO<sub>2</sub> (closed circles). Broken line in (C) and (F) represents phases of daylight (space) and darkness (line) during the experiments.

from T0 to T48 and T0 was significantly higher compared to the control and the CO<sub>2</sub> treatment (Fig. 7, Table 2). For individual Exp.'s, there was no significant difference between treatments for both *Synechococcus* spp. and *Prochlorococcus* spp. in Exp. I, II and III (Fig. 7).

From the microscopy samples, there was no significant difference in diatoms biomass between treatments during Exp.'s II and III (Table 2). The total biomass in Exp.'s II was low 3.5 and 4.5 μg C L<sup>-1</sup> at 48 h in CO<sub>2</sub> and control treatments, respectively when *Navicula* spp. accounted for the highest biomass. In Exp. II, the diatom biomass was higher and 17 and 18 μg C L<sup>-1</sup> in CO<sub>2</sub> and control treatments, respectively when *Rhizosolenia* spp. and *Navicula* spp. dominated (Fig. 8A and B). In this Exp. *Navicula* spp. dominated the biomass in the CO<sub>2</sub> treatment, whereas in the control *Rhizosolenia* spp. biomass was higher than any other group (Fig. 8A and B). The biomass of diatoms was significantly higher in T0 compared to both the control and CO<sub>2</sub> treatments (Fig. 8A and B, Table 2). The diatom biomass may have been reduced through silicate limitation.

Dinoflagellates exhibited the highest biomass of all phytoplankton groups during Exp.'s II and III, reaching on average 60 μg C L<sup>-1</sup> under CO<sub>2</sub> treatment and 30 μg C L<sup>-1</sup> in the control, though the differences between treatments were not significant (Table 2). *Gymnodinium* spp. accounted for the majority of the biomass, especially in Exp. III (Fig. 8D). The dinoflagellate biomass was also significantly higher in the control at T0 compared to T48, but this was not the case for the CO<sub>2</sub> treatment (Fig. 8C and D, Table 2). *T*-test

was not performed on individual Exp.'s, since only single samples were enumerated at T48.

### 3.4. Changes in photosynthesis and emission spectra

For all Exp.'s there was no significant difference in  $P_m^B$  between control and CO<sub>2</sub> treatment (Fig. 9A–C, Table 2). For the individual Exp.'s, there was no difference in  $P_m^B$  between control and CO<sub>2</sub> treatment in Exp. I (Fig. 9A), but  $P_m^B$  was significantly higher in the CO<sub>2</sub> treatment compared to the control in both Exp.'s II and III (Fig. 9B and C). In all Exp.'s,  $\alpha^B$  was significantly higher in the CO<sub>2</sub> treatment compared to the control (Fig. 9D–F, Table 2). There was no significant difference in  $\alpha^B$  in the control between T0 and T48, but  $\alpha^B$  was significantly higher at T48 in the CO<sub>2</sub> treatment compared to T0 (Table 2).

Using spectral de-convolution of LT emission spectroscopy measurements, the fluorescence peak at 678 nm is associated with uncoupled chlorophyll-containing PS antenna, while 686 nm represents a mixture of signals from PS II chlorophylls and terminal emitters of phycobilisomes (PBS) (Rakhimberdieva et al., 2007). Generally, the peak area at 678 nm decreased by more than three times from T0 to T48 in all Exp.'s and in both treatments (Fig. 10, Table 3). In all of the CO<sub>2</sub> treatments however, there was a significantly lower signal at 678 nm (Table 3), indicating reversible antenna connection after CO<sub>2</sub> enrichment. In addition, the spectral emission of the PSII core antenna increased from T0 to T48 (Fig. 10).

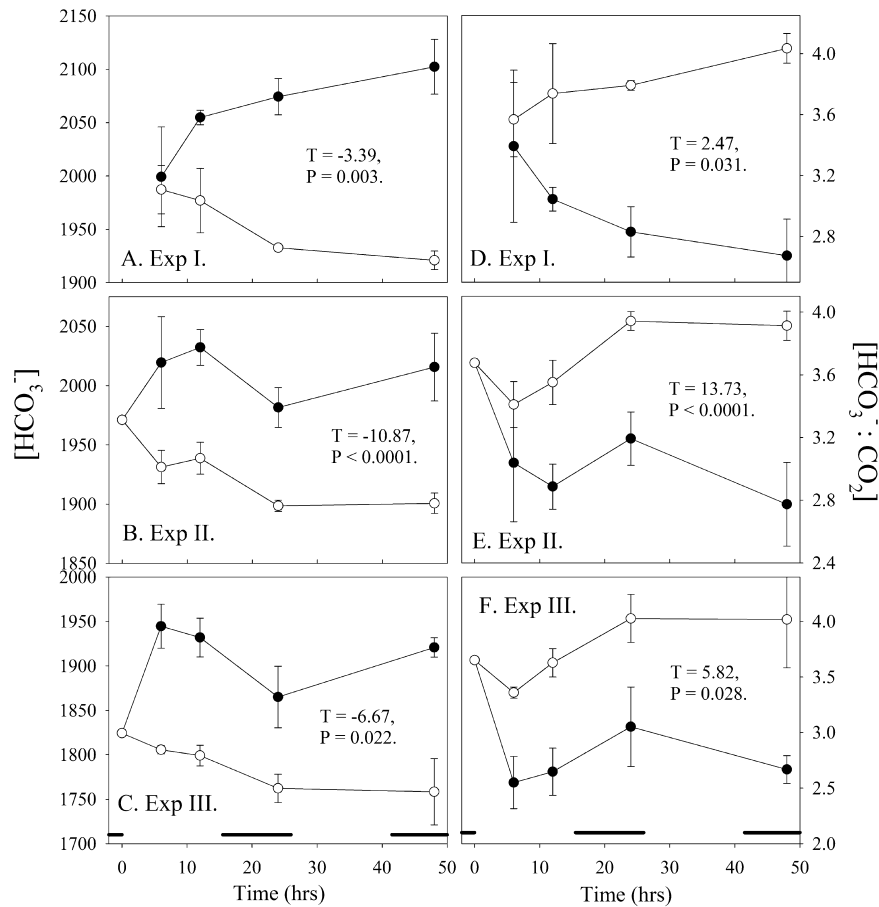


**Fig. 4.** Changes in  $HCO_3^-$  during experiments (A) I, (B) II, (C) III, and in  $HCO_3^- : CO_2$  during experiments (D) I, (E) II, (F) III in control (open circles) and 760 ppm  $CO_2$  (closed circles). Broken line in (C) and (F) represents phases of light (space) and dark (line) during the experiments.

**Table 1**  
Total alkalinity (TA) and total carbon (TC) for experiments I, II & III. SD is for N = 3.

Exp.	TA ( $\mu\text{mol L}^{-1}$ )	TC ( $\mu\text{mol kg}^{-1}$ )
<i>Exp. I</i>		
T0	2.488 $\pm$ 0.001	2212 $\pm$ 18
Control	2.495 $\pm$ 0.001	2169 $\pm$ 7
$CO_2$	2.517 $\pm$ 0.001	2294 $\pm$ 21
<i>Exp. II</i>		
T0	2.512 $\pm$ 0.002	2208 $\pm$ 2
Control	2.480 $\pm$ 0.001	2151 $\pm$ 7
$CO_2$	2.451 $\pm$ 0.008	2213 $\pm$ 23
<i>Exp. III</i>		
T0	2.338 $\pm$ 0.001	2048 $\pm$ 5
Control	2.316 $\pm$ 0.003	1992 $\pm$ 29
$CO_2$	2.304 $\pm$ 0.000	2101 $\pm$ 10

## 4. Discussion

### 4.1. Changes in the phytoplankton community in relation to carbonate chemistry

Experiments on  $CO_2$  enrichment of natural samples in the Atlantic Ocean have mostly focused on the interactions between diatoms, *Phaeocystis* spp. and prymnesiophytes. The sub-tropical and tropical oligotrophic gyres are dominated by Cyanobacteria which make a significant contribution to the carbon fixation in the global ocean (Bell and Kalff, 2001). In the North Atlantic gyre, the phytoplankton assemblage at the deep Chl *a* maximum is typically dominated by picoeukaryotes, *Prochlorococcus* spp. At the

DCM and *Synechococcus* spp. in the surface mixed layer (Tarran et al., 2006; Zubkov et al., 1998), which exist at very low (beyond detection limit) nitrate and phosphate concentrations. Under climate change scenarios of a warming ocean, increased stratification is likely to reduce nutrient concentrations in the sub-tropical gyres (Sarmiento et al., 2004). We conducted experiments with elevated  $CO_2$  in the North Atlantic sub-tropical gyre during autumn to evaluate the effects on phytoplankton community structure and photosynthetic rates. The Exp.'s were conducted with no nutrient addition to mimic the oligotrophic conditions of the gyre. The temperature at the experimental stations was 26–28 °C and typical of stratified sub-tropical waters where irradiance is high. During the Exp.'s, the phytoplankton community was dominated by dinoflagellates, which was 55–80 times higher than the other groups, but there was no significant difference between treatments and in some cases the biomass decreased from T0 to T48 (Fig. 8).

Understanding the response of dinoflagellates to both increases in  $CO_2$  and temperature is key to detecting climate-driven perturbations in the ecosystem. In culture experiments on autotrophic dinoflagellates, some strains of *Alexandrium fundyense* (Hattenrath-Lehmann et al., 2015), *Karenia brevis* (Errera et al., 2014), *Karlodinium veneficum* (Fu et al., 2010), *Prorocentrum minimum* and *Heterosigma akashiwo* (Fu et al., 2008) grow significantly faster at high  $pCO_2$ . Additionally, *Alexandrium fundyense* experiences a significant increase in cell toxicity under elevated  $CO_2$  (Hattenrath-Lehmann et al., 2015). There have been few studies on the response of *Gymnodinium* spp. and *Gyrodinium* spp., which exhibited high biomass in this study. Most *Gymnodinium* spp. are autotrophic, though some (e.g. *G. abbreviatum*, *G. heterostriatum*)

**Table 2**

Paired *T*-test for T0, control and CO<sub>2</sub> treatments for carbonate chemistry, phytoplankton community and photosynthetic parameters. df is degrees of freedom; T is the deviation of the sample mean from the normally distributed parametric mean to parametric standard deviation ratio, and P is the *T*-test critical significance value. Significant results are highlighted in bold.

Parameter	Variables	df	T	P
Carbonate CO <sub>2</sub>	<b>Chemistry</b>			
	<b>T0 v control</b>	<b>1, 9</b>	<b>4.92</b>	<b>0.001</b>
	<b>T0 v CO<sub>2</sub></b>	<b>1, 9</b>	<b>−9.43</b>	<b>&lt;0.0001</b>
pH	<b>Control v CO<sub>2</sub></b>	<b>1, 9</b>	<b>−11.84</b>	<b>&lt;0.0001</b>
	<b>T0 v control</b>	<b>1, 9</b>	<b>−2.89</b>	<b>0.02</b>
	<b>T0 v CO<sub>2</sub></b>	<b>1, 9</b>	<b>11.30</b>	<b>&lt;0.0001</b>
HCO <sub>3</sub> <sup>−</sup>	<b>Control v CO<sub>2</sub></b>	<b>1, 9</b>	<b>−13.55</b>	<b>&lt;0.0001</b>
	<b>T0 v control</b>	<b>1, 9</b>	<b>5.70</b>	<b>&lt;0.0001</b>
	<b>T0 v CO<sub>2</sub></b>	<b>1, 9</b>	<b>−3.91</b>	<b>0.004</b>
HCO <sub>3</sub> <sup>−</sup> :CO <sub>3</sub> <sup>2−</sup>	<b>Control v CO<sub>2</sub></b>	<b>1, 9</b>	<b>−11.84</b>	<b>&lt;0.0001</b>
	<b>T0 v control</b>	<b>1, 9</b>	<b>−4.30</b>	<b>0.003</b>
	<b>T0 v CO<sub>2</sub></b>	<b>1, 9</b>	<b>11.88</b>	<b>&lt;0.0001</b>
TC	<b>Control v CO<sub>2</sub></b>	<b>1, 9</b>	<b>−11.84</b>	<b>&lt;0.0001</b>
	T0 v control	1, 9	0.12	0.916
	T0 v CO <sub>2</sub>	1, 9	−1.36	0.307
TA	<b>Control v CO<sub>2</sub></b>	<b>1, 9</b>	<b>4.20</b>	<b>0.003</b>
	T0 v control	1, 9	0.13	0.312
	T0 v CO <sub>2</sub>	1, 9	0.83	0.496
Phytoplankton Chl <i>a</i>	Control v CO <sub>2</sub>	1, 9	0.16	0.881
	T0 v control	1, 9	0.11	0.912
	T0 v CO <sub>2</sub>	1, 9	0.12	0.909
Nano-eukaryotes	Control v CO <sub>2</sub>	1, 9	0.01	0.995
	T0 v control	1, 9	−0.65	0.533
	T0 v CO <sub>2</sub>	1, 9	0.63	0.543
Pico-eukaryotes	Control v CO <sub>2</sub>	1, 9	1.01	0.305
	T0 v control	1, 9	−1.19	0.268
	T0 v CO <sub>2</sub>	1, 9	0.83	0.430
<i>Synechococcus</i> spp.	Control v CO <sub>2</sub>	1, 9	0.92	0.382
	T0 v control	1, 9	1.50	0.271
	T0 v CO <sub>2</sub>	1, 9	1.45	0.285
<i>Prochlorococcus</i> spp.	Control v CO <sub>2</sub>	1, 9	0.82	0.500
	<b>T0 v control</b>	<b>1, 9</b>	<b>18.68</b>	<b>&lt;0.0001</b>
	<b>T0 v CO<sub>2</sub></b>	<b>1, 9</b>	<b>16.43</b>	<b>&lt;0.0001</b>
Diatoms	Control v CO <sub>2</sub>	1, 9	1.66	0.136
	<b>T0 v control</b>	<b>1, 6</b>	<b>2.63</b>	<b>0.046</b>
	<b>T0 v CO<sub>2</sub></b>	<b>1, 6</b>	<b>2.77</b>	<b>0.039</b>
Dinoflagellates	Control v CO <sub>2</sub>	1, 6	0.001	0.999
	<b>T0 v control</b>	<b>1, 6</b>	<b>1.77</b>	<b>0.327</b>
	T0 v CO <sub>2</sub>	1, 6	−0.49	0.711
Photosynthetic <i>p<sub>m</sub><sup>B</sup></i>	Control v CO <sub>2</sub>	1, 6	−1.61	0.354
	T0 v control	1, 3	3.06	0.092
	T0 v CO <sub>2</sub>	1, 3	0.26	0.819
<i>α<sup>B</sup></i>	Control v CO <sub>2</sub>	1, 3	−1.58	0.256
	T0 v control	1, 3	−1.09	0.319
	<b>T0 v CO<sub>2</sub></b>	<b>1, 3</b>	<b>−5.07</b>	<b>0.002</b>
77 K 678 nm	<b>Control v CO<sub>2</sub></b>	<b>1, 3</b>	<b>−4.40</b>	<b>&lt;0.002</b>
	T0 v control	1, 3	−0.07	0.951
	T0 v CO <sub>2</sub>	1, 3	0.25	0.824
77 K 686 nm	<b>Control v CO<sub>2</sub></b>	<b>1, 3</b>	<b>5.20</b>	<b>0.035</b>
	T0 v control	1, 3	1.13	0.374
	T0 v CO <sub>2</sub>	1, 3	0.77	0.522
77 K 691 nm	Control v CO <sub>2</sub>	1, 3	−2.00	0.184
	T0 v control	1, 3	−1.12	0.380
	T0 v CO <sub>2</sub>	1, 3	−1.20	0.353
77 K 711 nm	Control v CO <sub>2</sub>	1, 3	−2.00	0.184
	T0 v control	1, 3	4.00	0.057
	T0 v CO <sub>2</sub>	1, 3	1.39	0.300
	Control v CO <sub>2</sub>	1, 3	0.25	0.826

are known heterotrophs (Tomas, 1996). Similarly many *Gyrodinium* spp. are autotrophic, though some (e.g. *G. lachryma*, *G. pingue*, *G. spirale*) are heterotrophic (Tomas, 1996), so the patterns shown in Fig. 8C and D may also include some heterotrophs as we were not able to identify all *Gymnodinium* spp. and *Gyrodinium* spp. to species level. Calbet et al., 2014 studied the response of natural phytoplankton communities in a Norwegian Fjord using mesocosm experiments and found at elevated temperature and lower pH

there was no difference in *Gyrodinium* spp. abundance. Wynn-Edwards et al. (2014) found that in continuous batch culture of Antarctic strains of *Gymnodinium* spp. that there was no difference in growth rates and cell size between CO<sub>2</sub> enrichment to 993 ppm and ambient, but there was a significantly higher cell polyunsaturated fatty acid content at the higher CO<sub>2</sub> concentrations.

In our Exp.'s Diatoms had the second highest biomass, but there was no difference between the elevated CO<sub>2</sub> treatment and ambi-

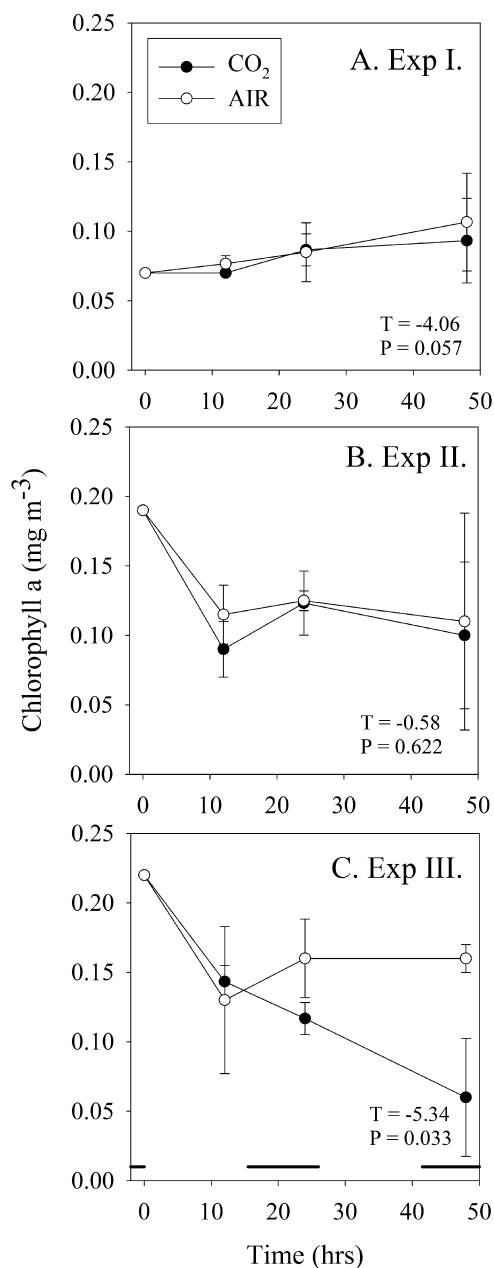


**Fig. 5.** Changes in Chlorophyll *a* during experiments (A) I, (B) II, (C) III. Broken line in (C) represents phases of light (space) and dark (line) during the experiments.

ent (Fig. 8, Table 2). In other studies, the growth rates of the diatoms *Skeletonema costatum* (Grev.) Cleve and *Chaetoceros* spp. increased at elevated CO<sub>2</sub> by 100% and 24%, respectively (Beardall and Raven, 2004; Kim et al., 2006). *Prochlorococcus* spp. exhibited the third highest biomass, however there was also no significant difference in the biomass of *Prochlorococcus* spp., and that of *Synechococcus* spp., picoeukaryotes, and nanoeukaryotes except in one Exp. III, in which there was a higher biomass of both picoeukaryotes and nanoeukaryote in the control (Fig. 6). The response of *Synechococcus* spp. in our experiments on natural samples contrasts the trends observed in culture experiments. For example, Fu et al. (2007) found that 750 ppm CO<sub>2</sub> stimulated the growth rate of *Synechococcus* spp. The different responses between *Synechococcus* spp. and *Prochlorococcus* spp. were thought to be due to differences in inorganic carbon acquisition systems associated with carbon limitation at low pCO<sub>2</sub> in *Synechococcus* spp.

(Fu et al., 2007). In contrast, we observed no difference in biomass between treatments under limiting nutrients. Similarly in natural phytoplankton communities Lomas et al. (2012) found that under replete P and Fe there was no significant response in the carbon-fixation of *Prochlorococcus* and *Synechococcus* spp. dominated communities to elevated CO<sub>2</sub> and a decrease in pH. In their study, pH was adjusted by acid-base manipulation (rather than direct enrichment with CO<sub>2</sub>) and nutrient media were added to the incubations even though nitrate and phosphate concentrations were below detection on first collection of the samples. By contrast, in mesocosm exp.'s using natural phytoplankton communities with replete nutrient concentrations, Paulino et al. (2008) reported a lower abundance of *Synechococcus* spp. and a higher abundance of picoeukaryotes at high CO<sub>2</sub>. By contrast, Low-Decarie et al. (2011) found in experimental mesocosms that increases in CO<sub>2</sub> enhanced the competitive ability of chlorophytes relative to cyanobacteria. Similarly in the North Atlantic, Feng et al. (2009) suggested that nanophytoplankton (coccolithophores) may further increase in abundance relative to other phytoplankton groups in the later stages of the spring bloom if future CO<sub>2</sub> concentrations and sea temperature continue to rise.

During our Exp.'s, dinoflagellates, diatoms and *Prochlorococcus* spp. decreased from the initial TO biomass, which may in part be due to the nitrate and silicate limitation or grazing by heterotrophic and/or mixotrophic dinoflagellates, through confinement in bottles. Nitrate and nitrite were low prior to confinement in all Exp.'s (Fig. 2) and silicate was beyond the detection limit. The limited silicate availability meant that biomass of diatoms was low, though it did increase in Exp. III. The biomass at TO suggests that the cyanobacteria were adversely affected by containment, which may have allowed the other groups to thrive due to lack of competition and/or the recycled nutrients released during the decline of the cyanobacteria biomass. Despite the initial decline, there was no clear response to elevated CO<sub>2</sub> in the phytoplankton assemblage. Most studies on changes in the phytoplankton community to elevated CO<sub>2</sub> report significant shifts or responses, however this may provide a biased view since non-significant responses are rarely published (Lomas et al., 2012).

#### 4.2. Effects of CO<sub>2</sub> enrichment on phytoplankton photosynthesis and primary production

Aquatic photosynthesis is inherently under-saturated with respect to CO<sub>2</sub> (Tortell et al., 2000), therefore increases in seawater CO<sub>2</sub> can enhance photosynthetic carbon fixation (Riebesell, 2004). Some studies have observed a 40% increase in the uptake of DIC at elevated CO<sub>2</sub> compared to present levels (Riebesell et al., 2007). It has been suggested that the photosynthesis of dinoflagellates may be limited by current water column CO<sub>2</sub> concentrations and that they may benefit from rising atmospheric pCO<sub>2</sub> (Eberlein et al., 2014). There are a number of studies that contradict this hypothesis, for example, in dilute batch cultures of the calcareous dinoflagellate *Scrippsiella trochoidea* and the toxic dinoflagellate *Alexandrium tamarense* grown at a range of CO<sub>2</sub> concentrations (180–1200 ppm), there was no significant difference in photosynthetic and growth rates between treatments, though *A. tamarense* did exhibit greater respiration rates at higher pCO<sub>2</sub> (Eberlein et al., 2014). In our experiments, photosynthetic rates were significantly greater in the CO<sub>2</sub> enriched treatment (Fig. 9) and the dinoflagellates were probably able to maximise carbon fixation due to lack of competition, since the biomass of the other groups was low (Figs. 6–8A and B). In Exp.'s II and III, when the dinoflagellates *Gymnodinium* and *Gyrodinium* spp. dominated the biomass, significantly higher  $P_m^B$  and  $\alpha^B$  at elevated CO<sub>2</sub> were associated with a lower signal of unconnected PS antennae, suggesting that these

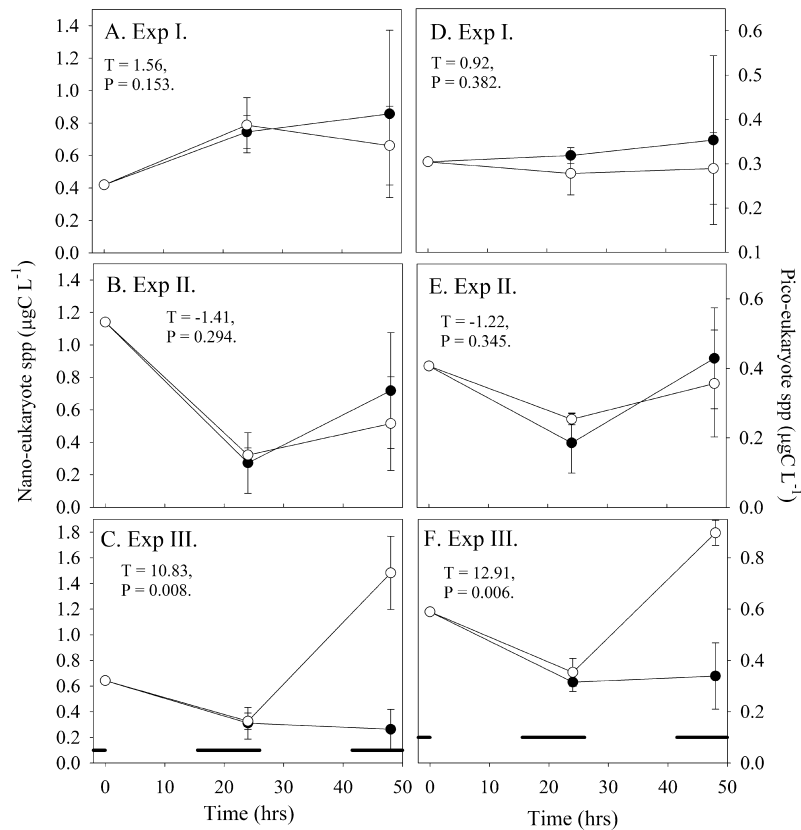


**Fig. 6.** Changes in the biomass of nano-eukaryotes in experiments (A) I, (B) II, (C) III, and changes in biomass of pico-eukaryotes in experiments (D) I, (E) II, (F) III in control (open circles) and 760 ppm CO<sub>2</sub> (closed circles). Broken line in (C) and (F) represents phases of light (space) and dark (line) during the experiments.

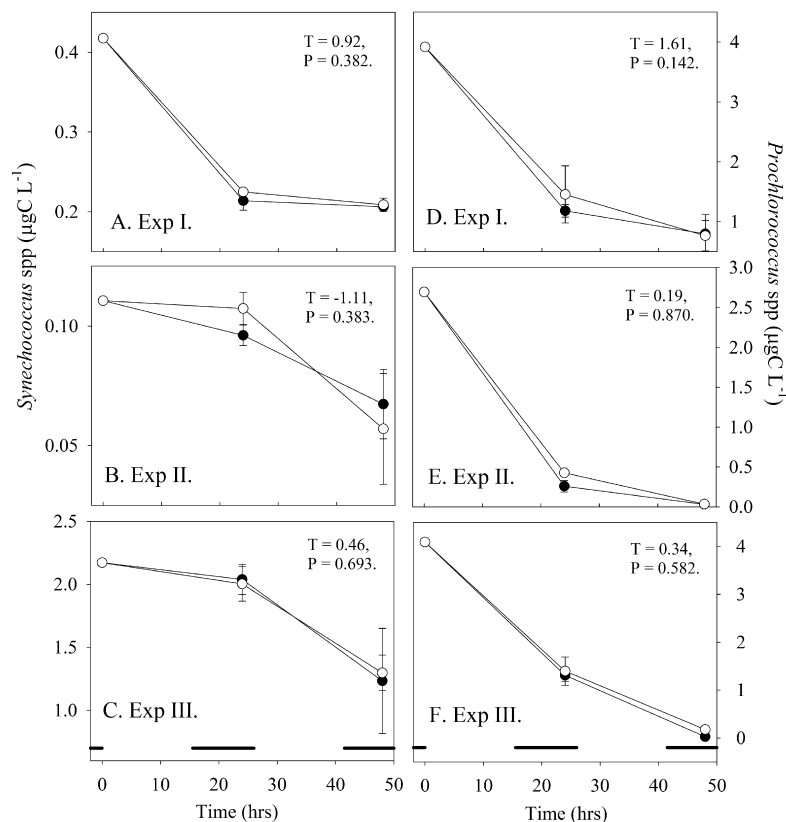


**Fig. 7.** Changes in the biomass of *Synechococcus* spp. in experiments (A) I, (B) II, (C) III, and changes in biomass of *Prochlorococcus* spp. in experiments (D) I, (E) II, (F) III in control (open circles) and 760 ppm CO<sub>2</sub> (closed circles). Broken line in (C) and (F) represents phases of light (space) and dark (line) during the experiments.

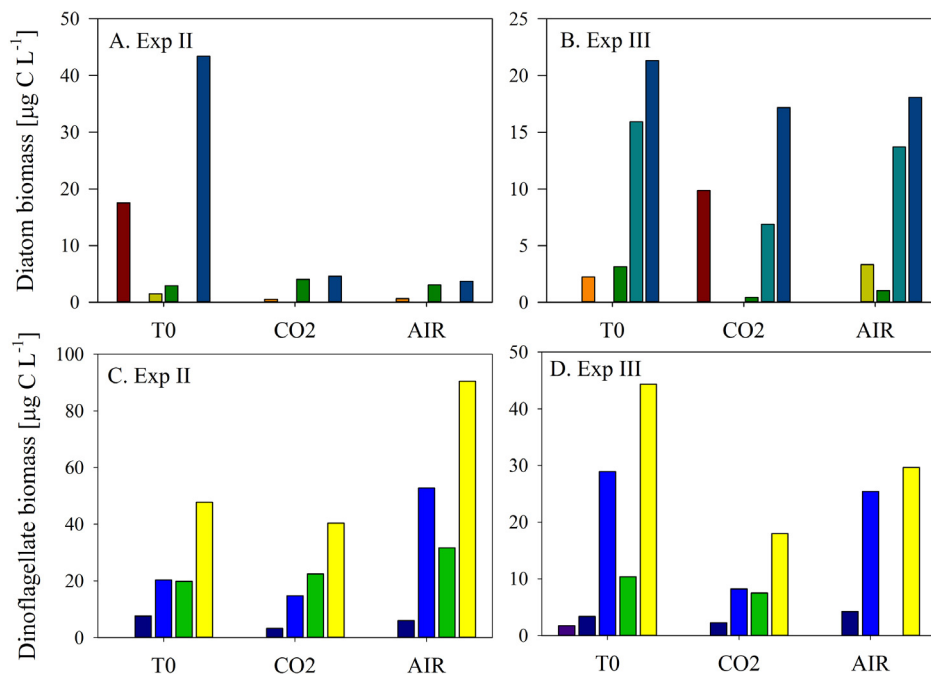


**Fig. 8.** Changes in diatom biomass during experiments (A) II and (B) III, and dinoflagellate biomass during experiments (C) II and (D) III at time (T) 0 and 48 h in control (AIR) and 760 ppm CO<sub>2</sub> enrichment. In (A) and (B) brown is *Navicula* spp., orange is pennate diatoms, light green is *Nitzschia* spp., dark green is *Thalassiosira* spp., light blue is *Rhizosolenia* spp. and dark blue is total diatom biomass. In (C) and (D) black is *Amphidinium* spp., dark blue is *Gonyaulax* spp., light blue is *Gymnodinium* spp., green is *Gyrodinium* spp., yellow is total dinoflagellate biomass (N = 1; microscope transects = 4).

previously unconnected PS antennae became connected to facilitate the higher photosynthetic rates. In addition, there was also a slight increase in fluorescence signal at 686 nm, due to a lower abundance of *Prochlorococcus* spp. in the CO<sub>2</sub> treatment compared to the control, since this group do not have PBS antennae (Partensky et al., 1999).

Photosynthetic carbon fixation is mediated by both pH and temperature dependent enzymatic reactions via the Calvin-Benson Cycle (Giordano et al., 2005; Portis and Parry, 2007). Varying climate change scenarios of increased CO<sub>2</sub>, temperature and a decrease in pH may affect intra-cellular DIC uptake differently in different phytoplankton groups or species (Badger et al., 1998).  $P_m^B$  and  $\alpha^B$  and temperature are tightly coupled (Uitz et al., 2008), and different phytoplankton species are adapted to a narrow temperature band with sharp decrease in photosynthetic rates beyond 20 °C (Eppley, 1972; Raven and Geider, 1988) which can be modified through the synthesis of photoprotecting rather than photosynthetic pigments (Kiefer and Mitchell, 1983). The enzyme that is primarily responsible for photosynthetic carbon fixation is Ribulose Bisphosphate Carboxylase (RuBisCO), though this does have some catalytic limitations (Giordano et al., 2005). Phytoplankton have therefore adapted two strategies to maximise the performance of RuBisCO; by either altering the affinity of RuBisCO or through CO<sub>2</sub>-concentrating mechanisms (CCMs). CCMs have a higher affinity for inorganic carbon (Giordano et al., 2005; Raven, 2011a,b; Reinfelder, 2011; Tortell et al., 2000), and through a combination of RuBisCO activity or CCM, most species achieve photosynthetic saturation at environmental CO<sub>2</sub> levels under light and nutrient replete conditions (Raven, 1997; Raven and Johnston, 1991). The differences in photosynthetic efficiency and rates between different phytoplankton groups can be partially explained by CCM and/or RuBisCO kinetics (Raven, 1997). The effect of an increase in CO<sub>2</sub> and decrease in pH may select phytoplankton species or genotypes based on the efficiency of RuBisCO or CCM. Dinoflagellates possess Form II RuBisCO (Morse et al., 1995), which

has low kinetic properties and therefore a low photosynthetic efficiency (Tortell et al., 2000). They are abundant in low nutrient oceanic waters (Margalef, 1979), have low growth rates attributed to their high basal respiration rates (Tang, 1996), do not need to compete for their position in the ecosystem and therefore rely on diffusive CO<sub>2</sub> uptake (Giordano et al., 2005). Dinoflagellates possess less efficient CCMs and/or low affinities for CO<sub>2</sub>, and may therefore benefit from living in a high CO<sub>2</sub> world (Reinfelder, 2011; Fu et al., 2012) and be highly sensitive to CO<sub>2</sub> (Rost et al., 2008). Form II RuBisCO has a much lower selectivity for CO<sub>2</sub> over O<sub>2</sub> (Giordano et al., 2005). To compensate for this, some marine dinoflagellates, such as *Prorocentrum minimum*, *Heterocapsa triquetra*, *Ceratium lineatum*, *Protoceratium reticulatum* and *Peridinium gatunense* have a CCM linked to carbonic anhydrases (CAs), the expression of which changes in response to the external CO<sub>2</sub> concentration (Berman-Frank et al., 1998; Brading et al., 2011; Ratti et al., 2007; Rost et al., 2006). This suggests that an increase in CO<sub>2</sub> stimulated efficiency in light absorption and utilization, which resulted in the higher rates of carbon fixation shown in Fig. 9. Using spectral de-convolution of low temperature emission spectroscopy measurements, the peak at 691 nm is emitted from active PS II chlorophylls and 711 nm from PS I chlorophylls (Kaňa et al., 2012). The fluorescence peak at 678 nm was assigned to uncoupled chlorophyll-containing PS antenna, while 686 nm represents a mixture of signals from PS II chlorophylls and terminal emitters of phycobilisomes (PBS) (Rakhimberdieva et al., 2007). The peak at 686 nm increased by a factor of two in all Exp.'s, which indicates either an increase in PBS content or the presence of the iron-stress protein, IsiA (Chauhan et al., 2011). The lower signal of unconnected PS antennae in our Exp.'s maybe indicative of CCM functionality as the dominant dinoflagellates connect more antennae to PS II to achieve the higher  $P_m^B$  and  $\alpha^B$  rates. The PS I chlorophyll peak at 711 nm remained constant and there was no obvious difference between treatments (Fig. 10, Table 2). Although semi-quantitative, the advantage of LT spectroscopy is that when it is

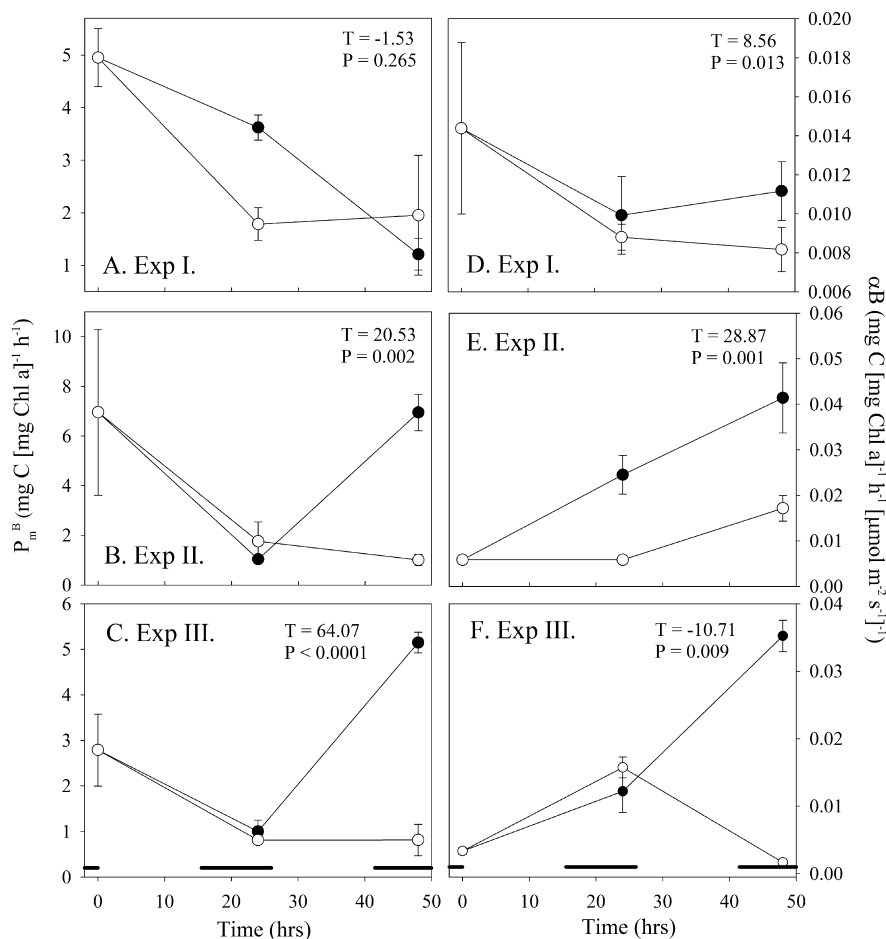


**Fig. 9.** Changes in  $P_m^B$  [mg C (mg Chl a)<sup>-1</sup> h<sup>-1</sup>] during experiments (A) I, (B) II and (C) III. Changes in  $\alpha B$  [mg C (mg Chl a)<sup>-1</sup> h<sup>-1</sup> ( $\mu\text{mol m}^{-2} \text{s}^{-1}$ )<sup>-1</sup>] during experiments (D) I, (E) II and (F) III. Broken line in (C) and (F) represents phases of light (space) and dark (line) during the experiments.

applied to time series and bioassays, gradual changes in phytoplankton photochemical processes can be monitored. This was the case in the Exp.'s on this cruise, where more detailed biochemical or biophysical analyses cannot usually be performed. Further work is required to ascertain whether the higher photosynthetic rates we observed in *Gymnodinium*, and *Gyrodinium* spp. under CO<sub>2</sub> enrichment is a species or genotypic response. This response also needs to be further investigated under different light conditions. For example, fluctuating light can affect dinoflagellate growth and photosynthesis with constant light and high CO<sub>2</sub> having a negative effect on the growth and quantum yield of *Prorocentrum micans* (Zheng et al., 2015), which has implications for ocean warming and high stratification in a high CO<sub>2</sub> world.

Cyanobacteria and chlorophytes possess Form IB RuBisCO (Badger and Price, 2003). Cyanobacteria utilize active HCO<sub>3</sub><sup>-</sup> and CO<sub>2</sub> pumps as their CCM to facilitate CO<sub>2</sub> fixation and maintain rapid growth at low external DIC concentrations (Badger and Price, 2003; Badger et al., 2006). In Exp. III, *Prochlorococcus* sp. biomass was significantly higher in the control, possibly as a result of their high affinity for CO<sub>2</sub> uptake at low concentrations or grazing of *Prochlorococcus* sp. biomass by heterotrophs or mixotrophs (Fig. 3D), but the photosynthetic rates in the control were significantly lower than the CO<sub>2</sub> treatment, principally because the dinoflagellate biomass was far higher in this Exp. By comparison, Fu et al. (2007) also observed that the photosynthetic rate and light harvesting efficiency of *Prochlorococcus* sp. *in vivo* was not affected by increasing CO<sub>2</sub>. Similar to the patterns we saw in Exp.'s II & III, Fu et al. (2007) also observed only slight differences in growth and

photosynthetic rates of *Synechococcus* spp. at 750 ppm CO<sub>2</sub> and control, though this changed when the temperature was elevated by 4 °C. By comparison, Lomas et al. (2012) observed that natural phytoplankton assemblages dominated by cyanobacteria were able to adapt to changes in pH through modification of the assimilation number, which resulted in no significant differences in photosynthetic rates. We found in two of our Exp.'s that the assimilation number was significantly higher at elevated CO<sub>2</sub>. The duration of our experiments represent short term responses to CO<sub>2</sub> enrichment and do not account for longer term adaptation and evolution, which can be complex (Collins and Bell, 2006). Our experiments also do not account for interactive synergies between CO<sub>2</sub>, temperature, nutrients and light which may affect phytoplankton, as shown by other studies in the North Atlantic (Feng et al., 2009; Hare et al., 2007). Further work is required to elucidate these dual effects on phytoplankton community structure in the North Atlantic sub-tropical gyre.

What is the consequence of increases in CO<sub>2</sub> on water column integrated primary production? Some studies have reported no significant changes in primary production under elevated CO<sub>2</sub> (Goldman, 1999; Raven and Falkowski, 1999; Tortell and Morel, 2002; Tortell et al., 2000). We found in the North Atlantic sub-tropical gyre when dinoflagellates dominated, that there was a 25% increase in primary production over all Exp.'s at 760 ppm CO<sub>2</sub> and that this was significant in Exp.'s II & III (Fig. 11). This is similar to the findings of Hein and Sand-Jensen (1997) who suggested that increasing CO<sub>2</sub> concentrations in seawater would increase primary production by 15–19%.

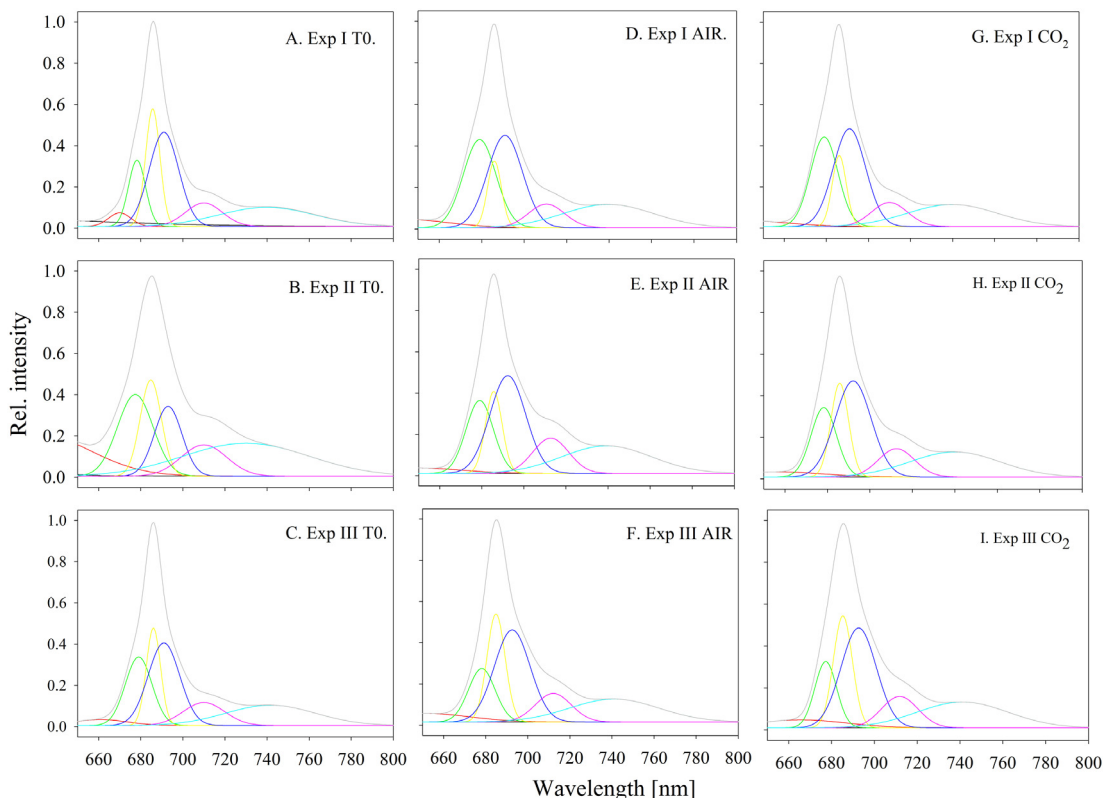


**Fig. 10.** Changes in low temperature emission during experiment (A) I CO<sub>2</sub> treatment, (B) I control, (C) II CO<sub>2</sub> treatment, (D) II control, (E) III CO<sub>2</sub> treatment, and (F) III control (N = 1). Spectra are: black – phycoerythrin; red – phycocyanin; light green – unconnected antenna; dark-blue – photosystem (PS) II or phycobilisomes anchoring pigments; yellow – PSII core antenna; cyanin – PSI; light-blue – vibrational peak; grey – cumulative sum of all spectra. (For interpretation of the references to colour in this figure legend, the reader is referred to the web version of this article.)

**Table 3**

The relative contribution of individual bands at different wavelengths from low temperature emission spectra after deconvolution. The band areas were calculated for the region 660–740 nm and the sum of all bands in this range equals 100%.

% Peak area	Exp I	Exp II	Exp III
<b>678 nm</b>			
T0	17	ND	27
Control	37	25	19
CO <sub>2</sub>	33	22	17
<b>686 nm</b>			
T0	26	ND	21
Control	12	17	25
CO <sub>2</sub>	13	21	26
<b>691 nm</b>			
T0	43	ND	39
Control	41	43	43
CO <sub>2</sub>	42	44	43
<b>711 nm</b>			
T0	13	ND	14
Control	11	16	13
CO <sub>2</sub>	12	13	14

## 5. Conclusions

Three CO<sub>2</sub> enrichment experiments were conducted on natural phytoplankton assemblages in the North Atlantic sub-tropical gyre. The dinoflagellates, *Gymnodinium*, and *Gyrodinium* spp., dominated the biomass but there was no significant difference in the biomass of these and other phytoplankton groups at elevated CO<sub>2</sub> concentrations of 760 ppm and 7.94 pH compared to ambient (468 ppm CO<sub>2</sub> and 8.33 pH). There were however, significantly higher photo-

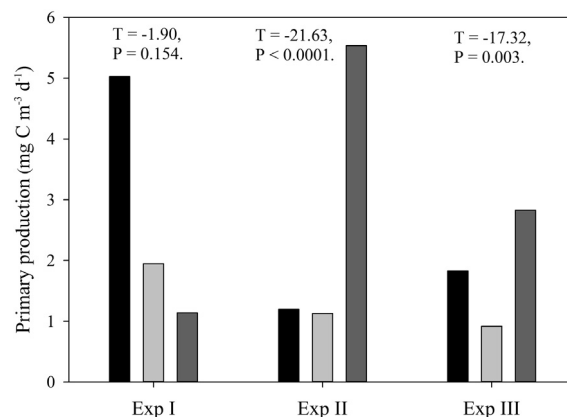


**Fig. 11.** Changes in Primary production [ $\text{mg C m}^{-3} \text{d}^{-1}$ ] at T0 (black bars), 48 h in control (light grey bars) and 760 ppm CO<sub>2</sub> (dark grey bars) for experiments I–II.

synthetic rates in the elevated CO<sub>2</sub> treatment which was due to the connection of reversible photosystem antennae at higher CO<sub>2</sub> concentrations, which resulted in a 25% increase primary production.

## Acknowledgements

We thank the Master and the Crew of the *RRS James Cook* for their help during AMT20 (cruise JC053). The training on alkalinity analysis by Dr. Helen Findlay is gratefully acknowledged. We also thank the Natural Environment Research Council (NERC) Earth Observation Data Acquisition and Analysis Service (NEODAAS) at Plymouth Marine Laboratory for supplying satellite imagery to

the ship. We are grateful to Dr. Rob Thomas for supplying Chl *a* data and to Carolyn Harris and Malcolm Woodward for the nutrient data shown in Fig. 2. G.H.T. and G.A.T. were supported by the Natural Environment Research Council's National Capability – The Atlantic Meridional Transect (AMT) and Oceans 2025 Theme 10a. B.S. was supported by a fellowship from the Partnership for Observations of the Global Oceans (POGO), for training on board RRS *James Cook* during AMT20. B.S., O.P. and R.K. were supported by GACR 206/08/1683 and the project Algatech CZ1.05/2.1.00/03.01/0110. This study is a contribution to the International IMBER project and is AMT contribution number 210.

## References

- Alley, R.B., Berntsen, T., Bindoff, N.L., Chen, Z., et al., 2007. Summary for Policymakers. Cambridge University Press, Cambridge and New York.
- Badger, M.R., Andrews, T.J., Whitney, S.M., Ludwig, M., Yellowlees, D.C., Leggat, W., Price, G.D., 1998. The diversity and coevolution of Rubisco, plastids, pyrenoids, and chloroplast-based CO<sub>2</sub>-concentrating mechanisms in algae. *Can. J. Bot.-Rev. Can. De Bot.* 76, 1052–1071.
- Badger, M.R., Price, G.D., 2003. CO<sub>2</sub> concentrating mechanisms in cyanobacteria: molecular components, their diversity and evolution. *J. Exp. Bot.* 54, 609–622.
- Badger, M.R., Price, G.D., Long, B.M., Woodger, F.J., 2006. The environmental plasticity and ecological genomics of the cyanobacterial CO<sub>2</sub> concentrating mechanism. *J. Exp. Bot.* 57, 249–265.
- Beardall, J., Raven, J.A., 2004. The potential effects of global climate change on microalgal photosynthesis, growth and ecology. *Phycologia* 43, 26–40.
- Bell, T., Kalff, J., 2001. The contribution of picophytoplankton in marine and freshwater systems of different trophic status and depth. *Limnol. Oceanogr.* 46, 1243–1248.
- Berman-Frank, I., Erez, J., Kaplan, A., 1998. Changes in inorganic carbon uptake during the progression of a dinoflagellate bloom in a lake ecosystem. *Can. J. Bot.-Rev. Can. De Bot.* 76, 1043–1051.
- Bjørnsen, P.K., 1986. Automatic determination of bacterioplankton biomass by means of image analysis. *Appl. Environ. Microbiol.* 51, 1199–1204.
- Booth, B.C., 1988. Size classes and major taxonomic groups of phytoplankton at two locations in the subarctic Pacific Ocean in May and August, 1984. *Mar. Biol.* 97, 275–286.
- Bopp, L., Monfray, P., Aumont, O., Dufresne, J.L., Le Treut, H., Madec, G., Terray, L., Orr, J.C., 2001. Potential impact of climate change on marine export production. *Global Biogeochem. Cycles* 15, 81–99.
- Brading, P., Warner, M.E., Davey, P., Smith, D.J., Achterberg, E.P., Suggett, D.J., 2011. Differential effects of ocean acidification on growth and photosynthesis among phylogenetic Symbiodinium (Dinophyceae). *Limnol. Oceanogr.* 56, 927–938.
- Brewer, P.G., Riley, J.P., 1965. The automatic determination of nitrate in seawater. *Deep-Sea Res.* 12, 765–772.
- Calbet, A., Sazhin, A.F., Nejtgaard, J.C., Berger, S.A., Tait, Z.S., Olmos, L., Sousoni, D., Isari, S., Martinez, R.A., Bouquet, J.M., Thompson, E.M., Bamstedt, U., Jakobsen, H., 2014. Future climate scenarios for a coastal productive planktonic food web resulting in microplankton phenology changes and decreased trophic transfer efficiency. *PLoS ONE*, 9.
- Chauhan, D., Folea, I.M., Jolley, C.C., Kouril, R., Lubner, C.E., Lin, S., Kolber, D., Wolfesimon, F., Golbeck, J.H., Boekema, E.J., Fromme, P., 2011. A novel photosynthetic strategy for adaptation to low-iron aquatic environments. *Biochemistry* 50, 686–692.
- Collins, S., Bell, G., 2006. Evolution of natural algal populations at elevated CO<sub>2</sub>. *Ecol. Lett.* 9, 129–135.
- Dickson, A.G., Afghan, J.D., Anderson, G.C., 2003. Reference materials for oceanic CO<sub>2</sub> analysis: a method for the certification of total alkalinity. *Mar. Chem.* 80, 185–197.
- Dickson, A.G., Millero, F.J., 1987. A comparison of the equilibrium constants for the dissociation of carbonic acid in seawater media. *Deep-Sea Res. Part A – Oceanogr. Res. Papers* 34, 1733–1743.
- Doney, S.C., Lindsay, K., Fung, I., John, J., 2006. Natural variability in a stable, 1000-yr global coupled climate-carbon cycle simulation. *J. Clim.* 19, 3033–3054.
- Eberlein, T., de Waal, D.B.V., Rost, B., 2014. Differential effects of ocean acidification on carbon acquisition in two bloom-forming dinoflagellate species. *Physiol. Plant.* 151, 468–479.
- Egleston, E.S., Sabine, C.L., Morel, F.M.M., 2010. Revelle revisited: buffer factors that quantify the response of ocean chemistry to changes in DIC and alkalinity. *Global Biogeochem. Cycles*, 24.
- Elzenga, J.T.M., Prins, H.B.A., Stefels, J., 2000. The role of extracellular carbonic anhydrase activity in inorganic carbon utilization of *Phaeocystis globosa* (Prymnesiophyceae): a comparison with other marine algae using the isotopic disequilibrium technique. *Limnol. Oceanogr.* 45, 372–380.
- Eppley, R.W., 1972. Temperature and phytoplankton growth in the sea. *Fish. Bull.* 70, 1063–1085.
- Errera, R.M., Yvon-Lewis, S., Kessler, J.D., Campbell, L., 2014. Responses of the dinoflagellate *Karenia brevis* to climate change: pCO<sub>2</sub> and sea surface temperature. *Harmful Algae* 37, 110–116.
- Feng, Y., Hare, C.E., Leblanc, K., Rose, J.M., Zhang, Y., DiTullio, G.R., Lee, P.A., Wilhelm, S.W., Rowe, J.M., Sun, J., Nemcek, N., Gueguen, C., Passow, U., Benner, L., Brown, C., Hutchins, D.A., 2009. Effects of increased pCO<sub>2</sub> and temperature on the North Atlantic spring bloom. I. The phytoplankton community and biogeochemical response. *Mar. Ecol. – Prog. Ser.* 388, 13–25.
- Feng, Y., Warner, M.E., Zhang, Y., Sun, J., Fu, F.-X., Rose, J.M., Hutchins, D.A., 2008. Interactive effects of increased pCO<sub>2</sub>, temperature and irradiance on the marine coccolithophore *Emiliania huxleyi* (Prymnesiophyceae). *Eur. J. Phycol.* 43, 87–98.
- Flynn, K.J., Clark, D.R., Mitra, A., Fabian, H., Hansen, P.J., Glibert, P.M., Wheeler, G.L., Stoecker, D.K., Blackford, J.C., Brownlee, C., 2015. Ocean acidification with (de) eutrophication will alter future phytoplankton growth and succession. *Proc. Roy. Soc. B – Biol. Sci.*, 282.
- Fu, F.-X., Place, A.R., Garcia, N.S., Hutchins, D.A., 2010. CO<sub>2</sub> and phosphate availability control the toxicity of the harmful bloom dinoflagellate *Karlodinium veneticum*. *Aquat. Microb. Ecol.* 59, 55–65.
- Fu, F.X., Tatters, A.O., Hutchins, D.A., 2012. Global change and the future of harmful algal blooms in the ocean. *Mar. Ecol. Prog. Ser.* 470, 207–233. <http://dx.doi.org/10.3354/meps10047>.
- Fu, F.-X., Warner, M.E., Zhang, Y., Feng, Y., Hutchins, D.A., 2007. Effects of increased temperature and CO<sub>2</sub> on photosynthesis, growth, and elemental ratios in marine *Synechococcus* and *Prochlorococcus* (Cyanobacteria). *J. Phycol.* 43, 485–496.
- Fu, F.-X., Zhang, Y., Warner, M.E., Feng, Y., Sun, J., Hutchins, D.A., 2008. A comparison of future increased CO<sub>2</sub> and temperature effects on sympatric *Heterosigma akashiwo* and *Prorocentrum minimum*. *Harmful Algae* 7, 76–90.
- Giordano, M., Beardall, J., Raven, J.A., 2005. CO<sub>2</sub> concentrating mechanisms in algae: mechanisms, environmental modulation, and evolution. *Annu. Rev. Plant Biol.* 56, 99–131.
- Goldman, J.C., 1999. Inorganic carbon availability and the growth of large marine diatoms. *Mar. Ecol. – Prog. Ser.* 180, 81–91.
- Grasshoff, K., 1976. *Methods of Seawater Analysis*. Verlag, Chemie, Weinheim.
- Gregg, W.W., Carder, K.L., 1990. A simple spectral solar irradiance model for cloudless maritime atmospheres. *Limnol. Oceanogr.* 35, 1657–1675.
- Hare, C.E., Leblanc, K., DiTullio, G.R., Kudela, R.M., Zhang, Y., Lee, P.A., Riseman, S., Hutchins, D.A., 2007. Consequences of increased temperature and CO<sub>2</sub> for phytoplankton community structure in the Bering Sea. *Mar. Ecol. – Prog. Ser.* 352, 9–16.
- Harris, C., 2011. AMT20 Nutrients. In: Rees, A.P. (Ed.), AMT20 Cruise Report, RRS *James Cook* JC053. Plymouth Marine Laboratory, Plymouth, UK, p. 148.
- Hattenrath-Lehmann, T.K., Smith, J.L., Wallace, R.B., Merlo, L.R., Koch, F., Mittelsdorf, H., Golecki, J.A., Anderson, D.M., Gobler, C.J., 2015. The effects of elevated CO<sub>2</sub> on the growth and toxicity of field populations and cultures of the saxitoxin-producing dinoflagellate, *Alexandrium fundyense*. *Limnol. Oceanogr.* 60, 198–214.
- Hein, M., Sandjensen, K., 1997. CO<sub>2</sub> increases oceanic primary production. *Nature* 388, 526–527.
- Hinga, K.R., 2002. Effects of pH on coastal marine phytoplankton. *Mar. Ecol. – Prog. Ser.* 238, 281–300.
- Holm-Hansen, O., Lorenzen, C.J., Holmes, R.W., Strickland, J.D.H., 1965. Fluorometric determination of chlorophyll. *J. du Conseil Permanent Int. pour l'Exploration de la Mer.* 30, 3–15.
- Hopkinson, B.M., Dupont, C.L., Allen, A.E., Morel, F.M.M., 2011. Efficiency of the CO<sub>2</sub>-concentrating mechanism of diatoms. *Proc. Natl. Acad. Sci. USA* 108, 3830–3837.
- Houghton, R.A., 2001. Counting terrestrial sources and sinks of carbon. *Climatic Change* 48, 525–534.
- Ihnken, S., Roberts, S., Beardall, J., 2011. Differential responses of growth and photosynthesis in the marine diatom *Chaetoceros muelleri* to CO<sub>2</sub> and light availability. *Phycologia* 50, 182–193.
- IOC, 1994. Protocols for the Joint Global Ocean Flux Study (JGOFS) Core Measurements. *IOC Manuals and Guides*, vol. 29, p. 126.
- Kaňa, R., Kotabová, E., Komárek, O., Papageorgiou, G.C., Govindjee, Šedivá, B., Prášil, O., 2012. *Biochim. et Biophys. Acta – Bioenerg.* 1817 (8), 1237–1247.
- Kiefer, D.A., Mitchell, B.G., 1983. A simple, steady-state description of phytoplankton growth based on absorption cross-section and quantum efficiency. *Limnol. Oceanogr.* 28, 770–776.
- Kim, J.-M., Lee, K., Shin, K., Kang, J.-H., Lee, H.-W., Kim, M., Jang, P.-G., Jang, M.-C., 2006. The effect of seawater CO<sub>2</sub> concentration on growth of a natural phytoplankton assemblage in a controlled mesocosm experiment. *Limnol. Oceanogr.* 51, 1629–1636.
- King, A.L., Jenkins, B.D., Wallace, J.R., Liu, Y., Wikfors, G.H., Milke, L.M., Meseck, S.L., 2015. Effects of CO<sub>2</sub> on growth rate, C:N:P, and fatty acid composition of seven marine phytoplankton species. *Mar. Ecol. Prog. Ser.* 537, 59–69.
- Kirkwood, D.S., 1989. Simultaneous Determination of Selected Nutrients in Seawater. *ICES, CM*, p. 29.
- Leonardos, N., Geider, R.J., 2005. Elevated atmospheric carbon dioxide increases organic carbon fixation by *Emiliania huxleyi* (Haptophyta), under nutrient-limited high-light conditions. *J. Phycol.* 41, 1196–1203.
- Lomas, M.W., Hopkinson, B.M., Losh, J.L., Ryan, D.E., Shi, D.L., Xu, Y., Morel, F.M.M., 2012. Effect of ocean acidification on cyanobacteria in the subtropical North Atlantic. *Aquat. Microb. Ecol.* 66, 211–222.
- Low-Decarie, E., Fussmann, G.F., Bell, G., 2011. The effect of elevated CO<sub>2</sub> on growth and competition in experimental phytoplankton communities. *Glob. Change Biol.* 17, 2525–2535.
- Mantoura, R.F.C., Woodward, E.M.S., 1983. Optimization of the indophenol blue method for the automated-determination of ammonia in estuarine waters. *Estuar. Coast. Shelf Sci.* 17, 219–224.

- Margalef, R., 1979. Life forms of phyto plankton as survival alternatives in an unstable environment. *Oceanol. Acta* 1, 493–509.
- Mehrbach, C., Culberso, Ch., Hawley, J.E., Pytkowicz, R.M., 1973. Measurement of apparent dissociation-constants of carbonic-acid in seawater at atmospheric-pressure. *Limnol. Oceanogr.* 18, 897–907.
- Menden-Deuer, S., Lessard, E.J., 2000. Carbon to volume relationships for dinoflagellates, diatoms, and other protist plankton. *Limnol. Oceanogr.* 45, 569–579.
- Morse, D., Salois, P., Markovic, P., Hastings, J.W., 1995. A nuclear-encoded form-II rubisco in dinoflagellates. *Science* 268, 1622–1624.
- Nimer, N.A., Merrett, M.J., 1996. The development of a CO<sub>2</sub>-concentrating mechanism in *Emiliania huxleyi*. *New Phytol.* 133, 383–389.
- Partensky, F., Hess, E.R., Vaulot, D., 1999. *Prochlorococcus*, a marine photosynthetic prokaryote of global significance. *Microbiol. Mol. Biol. Rev.* 63, 106–127.
- Paulino, A.I., Egge, J.K., Larsen, A., 2008. Effects of increased atmospheric CO<sub>2</sub> on small and intermediate sized osmotrophs during a nutrient induced phytoplankton bloom. *Biogeosciences* 5, 739–748.
- Pierrot, D.E., Wallace, D.W.R., 2006. MS Excel Program Developed for CO<sub>2</sub> System Calculations. ORNL/CDIAC-105a., Carbon Dioxide Information Analysis Center, Oak Ridge National Laboratory, Department of Energy, Oak Ridge, Tennessee, USA.
- Platt, T., Gallegos, C.L., Harrison, W.G., 1980. Photoinhibition of photosynthesis in natural assemblage of marine phytoplankton. *J. Mar. Res.* 38, 687–701.
- Portis Jr., A.R., Parry, M.A.J., 2007. Discoveries in Rubisco (Ribulose 1,5-bisphosphate carboxylase/oxygenase): a historical perspective. *Photosynth. Res.* 94, 121–143.
- Rakhimberdieva, M.G., Vavilin, D.V., Vermaas, W.F.J., Elanskaya, I.V., Karapetyan, N. V., 2007. Phycobillin/chlorophyll excitation equilibration upon carotenoid-induced non-photochemical fluorescence quenching in phycobilisomes of the *Synechocystis* sp PCC 6803. *Biochim. Et Biophys. Acta-Bioenerg.* 1767, 757–765.
- Ratti, S., Giordano, M., Morse, D., 2007. CO<sub>2</sub>-concentrating mechanisms of the potentially toxic dinoflagellate *Protoceratium reticulatum* (Dinophyceae, Gonyaulacales). *J. Phycol.* 43, 693–701.
- Raven, J.A., 1997. Inorganic carbon acquisition by marine autotrophs. *Adv. Bot. Res. Classic Papers*, vol. 27, pp. 85–209.
- Raven, J.A., 2011a. Effects on marine algae of changed seawater chemistry with increasing atmospheric CO<sub>2</sub>. *Biol. Environ. – Proc. Roy. Irish Acad.* 111B, 1–17.
- Raven, J.A., 2011b. Inorganic carbon acquisition by eukaryotic algae: four current questions. *Photosynth. Res.* 106, 123–134.
- Raven, J.A., Falkowski, P.G., 1999. Oceanic sinks for atmospheric CO<sub>2</sub>. *Plant, Cell Environ.* 22, 741–755.
- Raven, J.A., Geider, R.J., 1988. Temperature and algal growth. *New Phytol.* 110, 441–461.
- Raven, J.A., Johnston, A.M., 1991. Mechanisms of inorganic-carbon acquisition in marine-phytoplankton and their implications for the use of other resources. *Limnol. Oceanogr.* 36, 1701–1714.
- Reed, R., 1977. On estimating insolation over the ocean. *J. Phys. Oceanogr.* 7, 482–485.
- Reinfelder, J.R., 2011. Carbon concentrating mechanisms in eukaryotic marine phytoplankton. In: Carlson, C.A., Giovannoni, S.J. (Eds.), *Annual Review of Marine Science*, vol. 3, pp. 291–315.
- Riebesell, U., 2004. Effects of CO<sub>2</sub> enrichment on marine phytoplankton. *J. Oceanogr.* 60, 719–729.
- Riebesell, U., 2008. Climate change – acid test for marine biodiversity. *Nature* 454, 46–47.
- Riebesell, U., Schulz, K.G., Bellerby, R.G.J., Botros, M., Fritsche, P., Meyerhoefer, M., Neill, C., Nondal, G., Oschlies, A., Wohlers, J., Zoellner, E., 2007. Enhanced biological carbon consumption in a high CO<sub>2</sub> ocean. *Nature* 450, 545–U510.
- Riebesell, U., Wolfgladrow, D.A., Smetacek, V., 1993. Carbon-dioxide limitation of marine-phytoplankton growth-rates. *Nature* 361, 249–251.
- Rost, B., Riebesell, U., Sultemeyer, D., 2006. Carbon acquisition of marine phytoplankton: effect of photoperiod length. *Limnol. Oceanogr.* 51, 12–20.
- Rost, B., Zondervan, I., Wolf-Gladrow, D., 2008. Sensitivity of phytoplankton to future changes in ocean carbonate chemistry: current knowledge, contradictions and research directions. *Mar. Ecol. – Prog. Ser.* 373, 227–237.
- Sarmiento, J.L., Slater, R., Barber, R., Bopp, L., Doney, S.C., Hirst, A.C., Kleypas, J., Matear, R., Mikolajewicz, U., Monfray, P., Soldatov, V., Spall, S.A., Stouffer, R., 2004. Response of ocean ecosystems to climate warming. *Global Biogeochem. Cycles*, 18.
- Shi, D., Li, W., Hopkinson, B.M., Hong, H., Li, D., Kao, S.-J., Lin, W., 2015. Interactive effects of light, nitrogen source, and carbon dioxide on energy metabolism in the diatom *Thalassiosira pseudonana*. *Limnol. Oceanogr.* 60, 1805–1822.
- Skirrow, G., 1975. The dissolved gases – carbon dioxide.
- Smyth, T.J., Tilstone, G.H., Groom, S.B., 2005. Integration of radiative transfer into satellite models of ocean primary production. *J. Geophys. Res. – Oceans*, 110.
- Suggett, D.J., Stambler, N., Prasil, O., Kolber, Z., Quigg, A., Vazquez-Dominguez, E., Zohary, T., Berman, T., Iluz, D., Levitan, O., Lawson, T., Meeder, E., Lazar, B., Bar-Zeev, E., Medova, H., Berman-Frank, I., 2009. Nitrogen and phosphorus limitation of oceanic microbial growth during spring in the Gulf of Aqaba. *Aquat. Microb. Ecol.* 56, 227–239.
- Tang, E.P.Y., 1996. Why do dinoflagellates have lower growth rates? *J. Phycol.* 32, 80–84.
- Tarran, G.A., Heywood, J.L., Zubkov, M.V., 2006. Latitudinal changes in the standing stocks of nano- and picoeukaryotic phytoplankton in the Atlantic Ocean. *Deep-Sea Res. Part II – Top. Stud. Oceanogr.* 53, 1516–1529.
- Tarran, G.A., Zubkov, M.V., Sleight, M.A., Burkill, P.H., Yallop, M., 2001. Microbial community structure and standing stocks in the NE Atlantic in June and July of 1996. *Deep-Sea Res. Part II-Top. Stud. Oceanogr.* 48, 963–985.
- Tilstone, G.H., Figueiras, F.G., Lorenzo, L.M., Arbones, B., 2003. Phytoplankton composition, photosynthesis and primary production during different hydrographic conditions at the Northwest Iberian upwelling system. *Mar. Ecol. – Prog. Ser.* 252, 89–104.
- Tomas, C.R., 1996. *Identifying Marine Diatoms and Dinoflagellates*. Academic press Inc, San Diego, California.
- Tortell, P.D., Morel, F.M.M., 2002. Sources of inorganic carbon for phytoplankton in the eastern Subtropical and Equatorial Pacific Ocean. *Limnol. Oceanogr.* 47, 1012–1022.
- Tortell, P.D., Payne, C.D., Li, Y., Trimborn, S., Rost, B., Smith, W.O., Riesselman, C., Dunbar, R.B., Sedwick, P., DiTullio, G.R., 2008. CO<sub>2</sub> sensitivity of Southern Ocean phytoplankton. *Geophys. Res. Lett.*, 35.
- Tortell, P.D., Rau, G.H., Morel, F.M.M., 2000. Inorganic carbon acquisition in coastal Pacific phytoplankton communities. *Limnol. Oceanogr.* 45, 1485–1500.
- Uitz, J., Huot, Y., Bruyant, F., Babin, M., Claustre, H., 2008. Relating phytoplankton photophysiological properties to community structure on large scales. *Limnol. Oceanogr.* 53, 614–630.
- Wu, Y., Gao, K., Riebesell, U., 2010. CO<sub>2</sub>-induced seawater acidification affects physiological performance of the marine diatom *Phaeodactylum tricorutum*. *Biogeosciences* 7, 2915–2923.
- Wynn-Edwards, C., King, R., Davidson, A., Wright, S., Nichols, P.D., Wotherspoon, S., Kawaguchi, S., Virtue, P., 2014. Species-specific variations in the nutritional quality of Southern Ocean phytoplankton in response to elevated pCO<sub>2</sub>. *Water* 6, 1840–1859.
- Zheng, Y., Giordano, M., Gao, K., 2015. The impact of fluctuating light on the dinoflagellate *Prorocentrum micans* depends on NO<sub>3</sub><sup>-</sup> and CO<sub>2</sub> availability. *J. Plant Physiol.* 180, 18–26.
- Zubkov, M.V., Sleight, M.A., Tarran, G.A., Burkill, P.H., Leakey, R.J.G., 1998. Picoplanktonic community structure on an Atlantic transect from 50 degrees N to 50 degrees S. *Deep-Sea Res. Part I – Oceanogr. Res. Papers* 45, 1339–1355.